DOE/ER/14404--1

TECHNICAL PROGRESS REPORT

1993 - 1996

Award Number: DE-FG03-93ER14404

Project Title: Supramolecular Structures for Photochemical Energy Conversion

Project Directors: J. Devens Gust, Jr., Thomas A. Moore, Ana L. Moore

Institution: Center for the Study of Early Events in Photosynthesis
Department of Chemistry and Biochemistry
Arizona State University, Tempe, AZ 852897-1604

Date: June, 1996

I. Table of Contents

II. Technical Progress Report, 1993 - 1996

A. Research Goals

This research project is concerned with the design, synthesis and study by photochemical and spectroscopic methods of complex molecular devices that mimic some important aspects of photosynthetic electron and energy transfer. Photosynthetic solar energy conversion is the ultimate energy source for essentially all life. In addition, most of society's energy needs are met by the legacy of ancient photosynthesis in the form of coal, petroleum, natural gas and other fossil fuels, and by photosynthetically produced biomass in the form of firewood, alcohol fuels, etc. Photosynthesis is one of the most durable and, in its early steps, most efficient solar conversion "technologies", and it is therefore not surprising that it has long been a dream of photochemists to synthesize artificial reaction centers that employ the basic chemistry and physics of photosynthesis to help meet our energy needs. This project is exploring one approach to the realization of this dream: the preparation and study of photochemically active multicomponent molecules containing combinations of three to five chromophores, electron donors and electron acceptors. Properly engineered molecules of this type can functionally mimic photosynthetic light harvesting (singlet-singlet energy transfer between chromophores), photoprotection from light-initiated singlet oxygen damage (triplet-triplet energy transfer from chlorophylls to carotenoid polyenes), and, most importantly, photoinduced multistep electron transfer to generate charge-separated states that preserve some of the photon energy as chemical potential.

During the last three years, progress has been made on several fronts, all of which are related to the overall goal. A biomimetic system based on carotenoid-porphyrin-quinone triads has been constructed that demonstrates photoinduced transmembrane charge separation which in turn drives transmembrane proton transfer. Overall, light energy is used to establish a transmembrane proton gradient. This is the first example of a functional mimic of the light-driven proton pumping that fuels photosynthetic organisms. Another investigation has focused on the use of proton transfer reactions to stabilize the initial products of photoinduced electron transfer and thereby increase the yield of long-lived charge separation. A third study has investigated the influence of rigid molecular geometries and short donor-acceptor separations on photoinduced electron transfer reactions. This work has produced a porphyrin-quinone dyad molecule whose photoinduced electron transfer rate is essentially independent of solvent, temperature, and changes in thermodynamic driving force under all conditions studied thus far. The unusual results obtained with this molecule have led to the investigation of the effects of donor-acceptor separation, steric hindrance, electronic coupling, and intramolecular motions on photoinduced electron transfer in dyads and triads. Finally, generation and quenching of singlet molecular oxygen by chlorophyll aggregates has been studied. Singlet oxygen, a byproduct of photosynthesis, can damage both natural and artificial photosynthetic systems.

B. Photochemical Energy Conversion by a Biomimetic Energy Transducing Membrane

Bilayer lipid membranes are essential components of living things. They are an integral part of cell walls and they serve to define and compartmentalize organelles. Membranes are important sites for energy transduction. From the standpoint of nanoscale energy-converting devices, bilayer lipid membranes may be viewed as an interface between the molecular scale and the macroscopic scale. Bilayer lipid membranes assembled into liposomes display these two scales in that liposomes have diameters in the range of several hundred nanometers to a few microns while their bilayer membrane thickness is about 5 nanometers. Therefore, the dimension of membrane thickness is of molecular scale and molecules can be designed to span the bilayer and carry out photochemistry and charge transport between the two separate aqueous phases. The aqueous phase external to the liposome is readily manipulated and probed by ordinary laboratory techniques. The aqueous phase contained in the interior of the liposome is defined by ordinary laboratory techniques prior to the formation of the liposome. After liposomes have formed, the interior phase is subject to modification through single-molecule or single-photon events mediated by molecules located in the bilayer.

The experiments carried out to date focus on liposome-based photochemical systems that mimic energy conservation in biological cells. The production of transmembrane electrochemical potential and its coupling to the generation of proton motive force is the unifying principle of membrane-linked bioenergetics. In photosynthetic organisms, transmembrane photoinduced electron transfer is carried out by pigments organized into reaction centers by membrane-spanning proteins. Other membrane-spanning proteins use quinones and other cofactors to couple the resulting redox potential gradient to the translocation of protons across the membrane.

Recently, artificial reaction centers have been synthesized that consist of electron donors and acceptors covalently linked together so that photoinduced electron transfer and subsequent thermal electron transfers separate charge over as much as 8 nm.[2,4,5] We have now assembled molecular triad artificial reaction centers and collateral quinones into a liposome-based model system that uses light energy to translocate protons across the bilayer. Upon excitation, electron transfer processes in the triad generate reduction potential near the outer surface of the bilayer and oxidation potential near the inner surface. In response to this vectorial redox potential gradient, a freely-diffusing quinone alternates between its oxidized and semiquinone forms to transport protons across the bilayer. These experiments demonstrate the conversion of light energy to transmembrane proton motive force in a purely synthetic, biomimetic system.

Molecular triad **1** was prepared by linking a synthetic tetraarylporphyrin (P) to both a *peri*-hydroxynaphthoquinone (Q) and a caroteniod polyene (C).[14] Upon excitation, triad **1** dissolved in various solvents undergoes photoinduced electron transfer from the excited singlet state of the porphyrin moiety to yield the intermediate charge-separated species C-$P^{\bullet+}$-$Q^{\bullet-}$ in less than 30 ps and with a quantum yield of ~1. Subsequent electron transfer from the carotenoid to the porphyrin radical cation competes with charge recombination to yield $C^{\bullet+}$-P-$Q^{\bullet-}$ with a quantum yield up to 0.2 and a lifetime of ~70 ns.[14]

Reverse-phase evaporation (RPE) liposomes were prepared by standard procedures using 5 mg of a 2:3 molar ratio of phosphatidylserine and dioleoylphosphatidylcholine. The solution also contained 0.05 M KCl and pyranine trisulfonate (PS), a water soluble dye that indicates pH by the ratio of the amplitude of the fluorescence excitation spectrum at 406 nm to that at 456 nm (I_{406}/I_{456}).

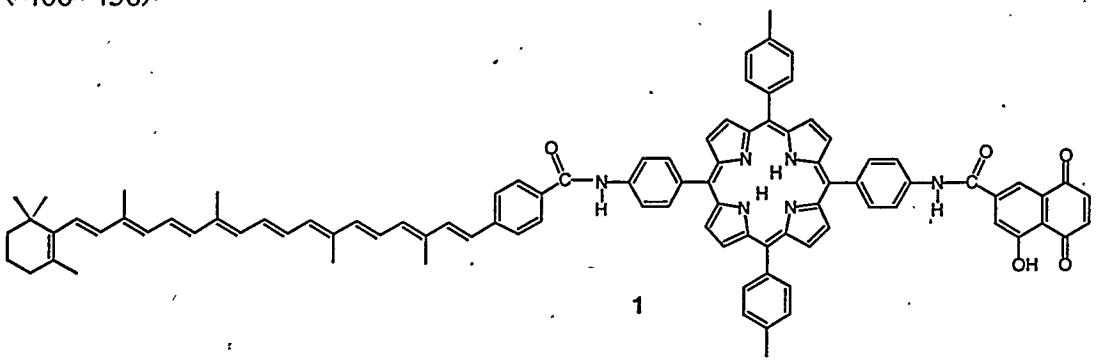

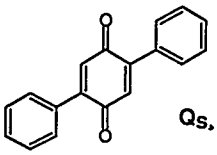

For certain experiments, the lipid mixture also contained 0.4 mg of lipid-soluble 2,5-diphenylbenzoquinone (Q_S) as the proton shuttle. The midpoint potential for the one-electron reduction of Q_S is more positive by 160 mV than that of the quinone component of **1**. In certain control experiments ubiquinone was used as the secondary quinone. Triad **1** was added to a stirred solution of liposomes by injection of 30 - 40 mL of a 7.7×10^{-2} mM solution of **1** in tetrahydrofuran. The liposomes were then purified by gel chromatography (Sephadex G-100) and eluted with a 0.05 M KCl solution. Quantitative analysis of the organic phosphorus in these liposomes indicated that they typically contained ~5×10^{17} molecules of lipid per mL. RPE liposomes formed in this way have ~8×10^4 molecules of lipid per liposome (therefore, ~5×10^{12} liposomes per mL), an average diameter of 100 nm and an average volume of 4×10^{-18} L. Based on the amount of dye and **1** extracted from a typical liposome preparation, there are ~40 molecules of **1** in the bilayer and ~50 molecules of PS in the interior aqueous phase of each liposome. The calculated amount of Q_S in the bilayer was ~900 molecules per liposome.

Vectorial electron and proton transport requires asymmetric insertion of the molecular triad artificial reaction center into the liposomal bilayer membrane. This was accomplished by injection of a tetrahydrofuran solution of **1** into an aqueous solution containing liposomes, a procedure which delivers **1** to the outside surface of the bilayer. The preference for the directional order indicated in Figure 1 is expected because insertion of the lipophilic carotenoid of **1** into the bilayer avoids the energetic cost of moving the polar, phenol-bearing quinone through the low dielectric medium.
Laser flash photolysis experiments on liposomes containing **1** support the liposome-triad structure illustrated in Figure 1. Excitation of the porphyrin moiety of **1** in liposomes with 5-ns laser pulses at 430 nm resulted in formation of $C^{\bullet+}$-P-$Q^{\bullet-}$, as detected by the strong transient absorbance of the carotenoid radical cation at 940 nm.[5] The lifetime of this

species was ~ 80 ns. Experiments on **1** in dichloromethane/water mixtures have established that $NaBH_4$ (or $Na_2S_2O_4$) reduces the quinone so that photoinduced electron transfer from the porphyrin singlet state does not occur. Under these conditions $C^{\bullet+}$-P-$Q^{\bullet-}$ does not form, as indicated by the lack of transient absorbance at 940 nm. Titration of liposomes containing **1** with $NaBH_4$ (or $Na_2S_2O_4$), which is not expected to cross the bilayer, decreased the yield of $C^{\bullet+}$-P-$Q^{\bullet-}$ monotonically to ~0 without quenching its lifetime. These experiments demonstrate that $NaBH_4$ (or $Na_2S_2O_4$) has access to the quinones at the outside bilayer-water interface, and suggest that because there was no residual carotenoid radical cation observed, the majority of the triads must be so disposed. The observation that the lifetime of $C^{\bullet+}$-P-$Q^{\bullet-}$ was not shortened upon addition of $NaBH_4$ (or $Na_2S_2O_4$) indicates that under these conditions reductant in the external aqueous phase does not have access to the carotenoid radical cation. In other words, both the yield and lifetime results are consistent with the structure shown in Figure 1 in which the majority of the triads are oriented so that the quinone is proximal to the external aqueous - liposome interface where it can be reduced prior to excitation, while the carotenoid is distal to that interface.

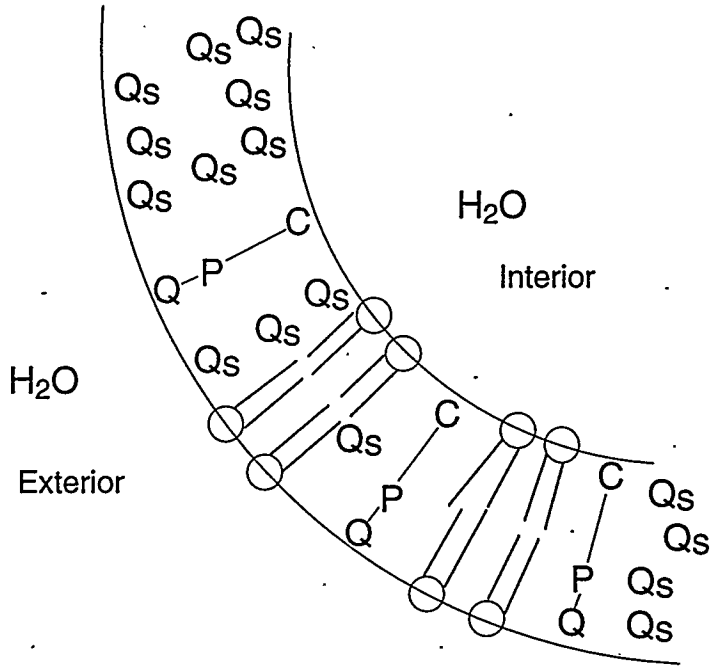

Figure 1. Schematic diagram illustrating the orientation of triad **1** in a liposome, with its quinone near the interface between the bulk aqueous phase and the bilayer lipid membrane. Q_S is shown dispersed in the hydrophobic phase of the bilayer.

Figure 2 presents the fluorescence excitation spectra of the pH-indicating dye PS contained inside the liposomes before and after irradiation of a solution of liposomes with a ~5 mW cm^{-2} beam of 650 nm light having a 10 nm bandpass. These liposomes contained **1** in the bilayer but did not contain the shuttle quinone Q_S. The two fluorescence excitation spectra are superimposable, indicating that there was no change in the protonation state of the dye as a result of irradiation. Exactly the same results were

obtained when liposomes that contained Q_S but no triad **1** were irradiated. Similarly, there was no change in the protonation state of the dye when liposomes containing both **1** and Q_S were kept in the dark or were irradiated at 780 nm (where **1** does not absorb). Also, there was no change in the protonation state of the dye when liposomes containing **1** but in which ubiquinone was substituted for Q_S were irradiated with 650 nm light. (The midpoint potential for reduction of ubiquinone is more negative than that of the quinone moiety of **1** by 440 mV.) Finally, liposomes containing **1** and Q_S, but which were treated with $NaBH_4$ prior to irradiation, were not photochemically active.

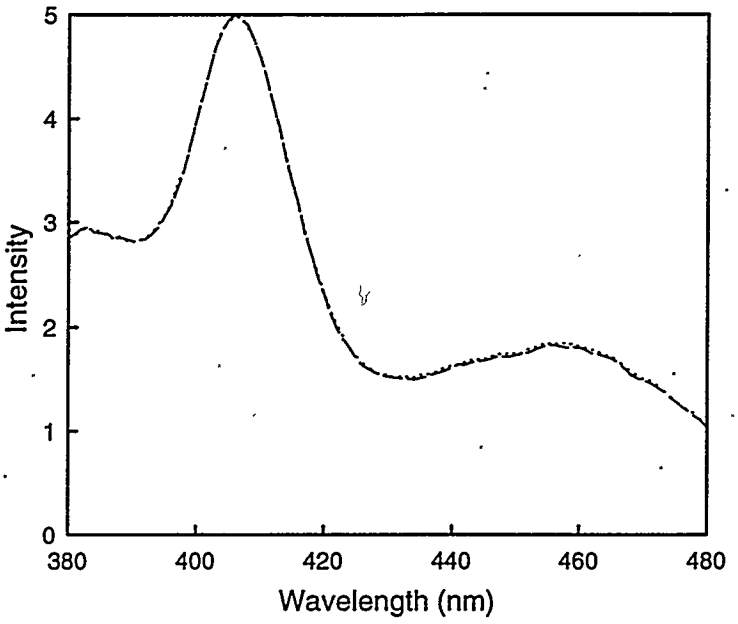

Figure 2. Excitation spectra for emission at 510 nm of PS inside liposomes containing **1**, but not Q_S, in the bilayer. The spectra before (– – – –) and after (• • • •) irradiation with 5 mW of 650 nm light for 10 min are essentially superimposable.

Figure 3 presents excitation spectra of PS in liposomes containing triad **1** and Q_S in the bilayer as a function of irradiation time. The increasing ratio of I_{406}/I_{456} with irradiation time indicates that the dye population is increasingly shifted toward the protonated form. Figure 4 presents the I_{406}/I_{456} ratio for this experiment as a function of irradiation time.

Experiments at fixed irradiation time and increased light intensity were also performed. Both types of experiments were linear with light dose in the initial phase, and approached saturation at high total photons absorbed. The change in protonation state of an irradiated sample after the addition of 1×10^{-7} moles of a proton ionophore (carbonyl cyanide *p*-(triflоromethoxy)phenylhydrazone (FCCP)) is also shown in Figure 4. The proton ionophore relaxes the protonation state of the dye to its level prior to irradiation.

These results demonstrate that in the presence of Q_S, light absorbed by **1** drives protons into the interior aqueous phase of the liposomes. A mechanism for proton translocation consistent with these experiments is presented in the elementary processes 1 - 7 illustrated in Figure 5.

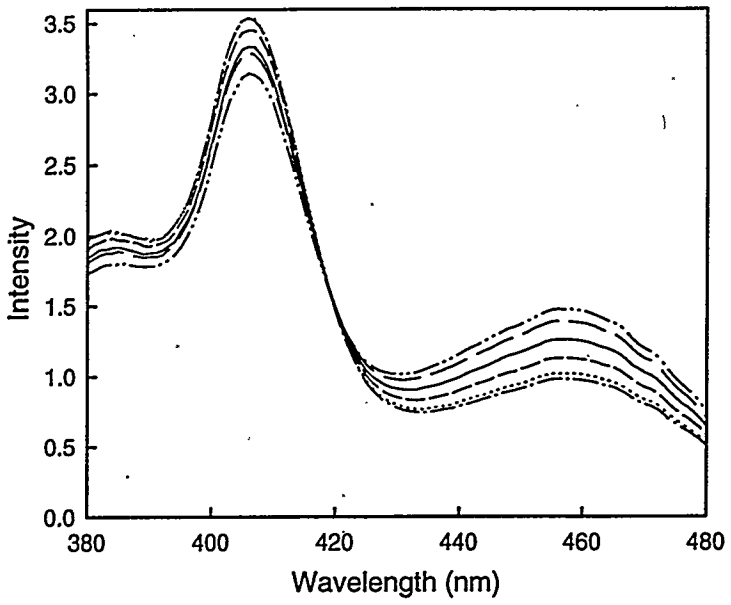

Figure 3. Excitation spectra for emission at 510 nm of PS inside liposomes containing **1** and shuttle quinone Q_S in the bilayer. The liposomes were irradiated for 0 (– • • – • • – • •), 5 (— — —), 18 (————), 38 (– – – –), 68 (• • • •), and 83 (– • – • – •) min with ~ 5 mW of 650 nm light.

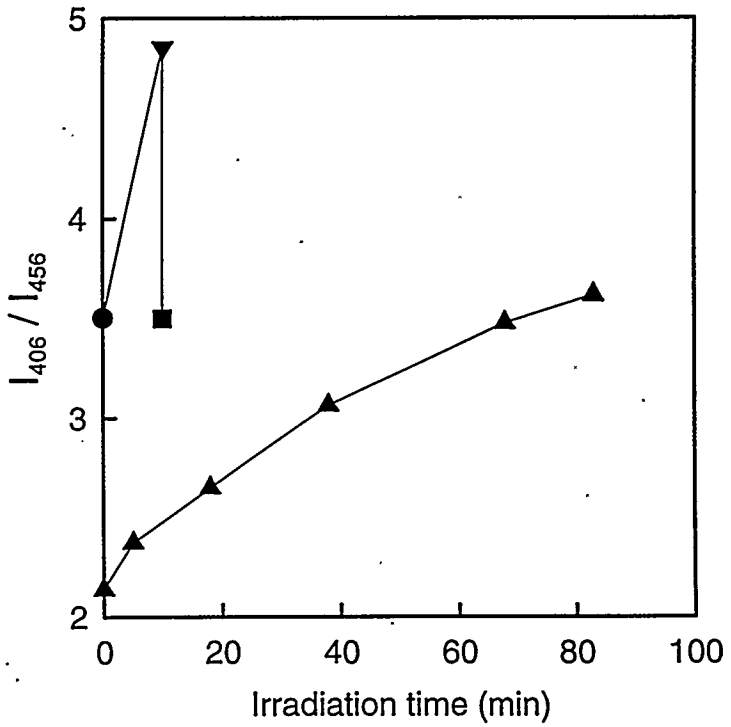

Figure 4. The ratio I_{406}/I_{456} from the data in Figure 3 plotted as a function of irradiation time (▲). In a different experiment, I_{406}/I_{456} before irradiation (●), after irradiation (▼), and after addition of 1×10^{-7} moles of FCCP (■).

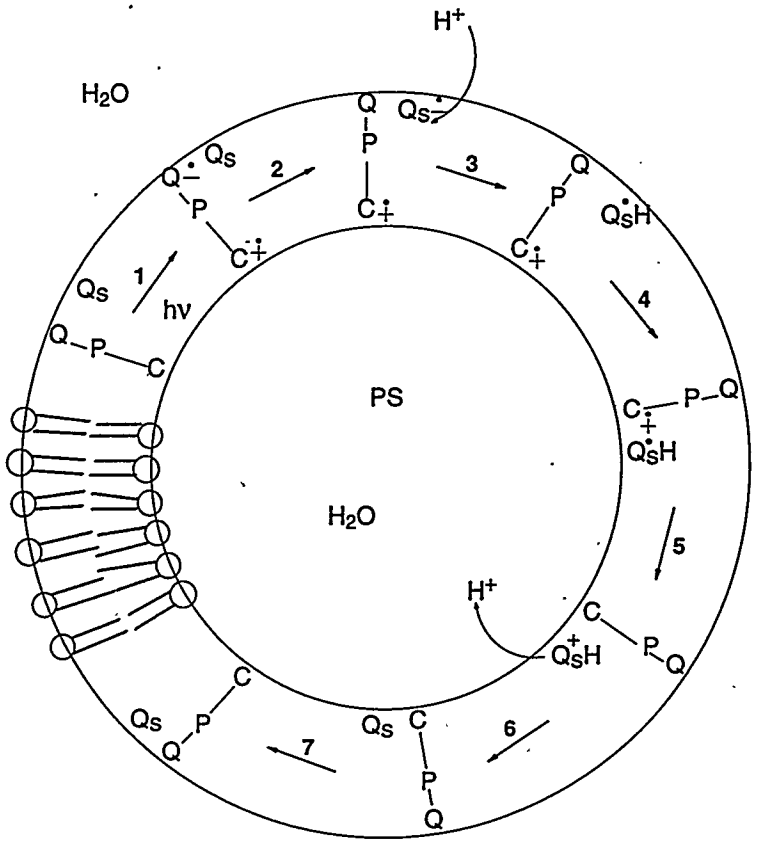

Figure 5. Proposed elementary processes involved in proton translocation across the liposome bilayer.

Step 1 includes excitation and two-step charge separation. Photoinduced electron transfer and subsequent formation of the carotenoid radical cation is confirmed by the transient absorbance at 940 nm of the $C^{\bullet+}$-P-$Q^{\bullet-}$ species, the observation that light of wavelengths absorbed by triad **1** is required, and the fact that proton translocation is not observed when the quinone moiety of **1** is reduced prior to excitation. In step 2, Q_S near the external aqueous phase accepts an electron from $C^{\bullet+}$-P-$Q^{\bullet-}$. This step is thermodynamically allowed and is consistent with the control experiments mentioned above where proton pumping was not observed in the absence of Q_S or with ubiquinone, in which case step 2 is endergonic. In step 3 the Q_S radical anion accepts a proton from the nearby external aqueous phase. This step is driven by the pK of $Q_S^{\bullet-}$ and forms the semiquinone, $Q_SH^{\bullet}$. (Protonation of the anion radical of **1** followed by electron transfer to Q_S and protonation would also yield $Q_SH^{\bullet}$.) Step 4 indicates the diffusion of $Q_SH^{\bullet}$ across the bilayer. $Q_SH^{\bullet}$ should be sufficiently nonpolar that it may cross the membrane to the region near the interior aqueous phase where the oxidizing potential is located. Step 5 depicts the oxidation of $Q_SH^{\bullet}$ by the radical cation of **1**, regenerating the photocatalyst. In step 6 the protonated quinone deprotonates with a driving force provided by its pKa of ~ – 6. Step 7 is included to illustrate the return of Q_S to the exterior region of the bilayer. The sum of steps 1 - 7 is photoinduced electron transfer that generates transmembrane redox potential which in turn drives the vectorial translocation of protons by a quinone shuttle.

In order to interpret changes in the excitation spectrum of PS in terms of the quantum yield of proton translocation, we have assumed a model for the response of PS to proton influx. Calculations show that the liposome interior volume is ~4×10^{-18} L, and consequently at neutral pH most of the liposomes contain no hydronium ions. The ratio of the number of protonated to unprotonated PS molecules trapped in the interior of a dye-containing liposome, (#HPS)/(#PS), is fixed by the pH of the aqueous phase in which the liposomes were formed and was calculated from pH = pK - log (#HPS)/(#PS). From this ratio and the average number of PS molecules per liposome (~50), #HPS and #PS were calculated. Even though addition of a single proton to the interior phase would increase the proton activity to ~pH 6.4 (in the absence of dye), the response of the dye is limited to a change in the above ratio to (#HPS + 1)/(#PS - 1). The excitation spectra ratio (I_{406}/I_{456}) expected from this change was determined by calculating the pH from pH = pK - log (#HPS + 1)/(#PS - 1) and finding the corresponding I_{406}/I_{456} ratio from an experimental titration curve of PS. This ratio, $(I_{406}/I_{456})_{max}$, would be observed if every liposome had one proton translocated into the interior. The observed I_{406}/I_{456} ratio at a short irradiation time (see Figure 4) divided by $(I_{406}/I_{456})_{max}$ gives the fraction of liposomes in which a proton was translocated. The number of photons absorbed to produce the initial change in I_{406}/I_{456} was measured and the quantum yield was estimated to be roughly 1×10^{-5}. This calculation ignores any buffering effect of the lipid.

The initial phase of this work has been submitted for publication.[16] The observation of a photogenerated change in the protonation level of the PS dye inside the liposomes which spontaneously relaxes upon addition of a proton ionophore demonstrates that transmembrane proton potential was generated and stored in these experiments. It is noteworthy that in this system photon energy is transduced into transmembrane redox potential and then into proton motive force by a chemically cyclic mechanism. That is, it does not require sacrificial electron acceptors or donors. Translocation of one proton into a liposome of this type generates a calculated proton motive force of >0.5 pH unit and a concomitant modest membrane potential. It is expected that proton motive force built up across membranes in this way can be harnessed in a variety of biomimetic, energy linked processes.

C. Stabilization of Charge Separation by Coupled Electron and Proton Transfer

1. Introduction

Natural photosynthetic reaction centers employ a multistep electron transfer strategy to achieve charge separation across membranes with a total quantum yield of near unity. Thus, at each intermediate step the forward electron transfer process dominates charge recombination. It is a significant challenge to design synthetic multicomponent electron transfer molecules in which photoinduced charge separation is followed by forward electron transfer processes that are much faster than electron-hole recombination. Previously, we have used thermodynamic and electronic principles to improve the yield of long-lived charge separation in donor-pigment-acceptor triad molecules, and have designed and synthesized devices having more than three components in which parallel forward electron transfer paths compete with recombination

to enhance the yield of the final charge-separated state.[2,4,5] In this section of the report we describe another approach, based on rapid proton transfer.

The simplest molecular system that can demonstrate multistep electron transfer is a triad. In the original carotene-porphyrin-quinone (C-P-Q) triad,[2] the porphyrin first excited singlet state C-^{1}P-Q donates an electron to the quinone to form C-P$^{\bullet+}$-Q$^{\bullet-}$. A second electron transfer, from the carotenoid, competes with charge recombination to the ground state yielding a final, long-lived C$^{\bullet+}$-P-Q$^{\bullet-}$ charge-separated state. Triad **2**, which features a naphthoquinone moiety with a fused norbornene skeleton bearing a carboxylic acid group at a bridgehead,[12,14] has been designed to incorporate a rapid, unimolecular proton transfer reaction (eq 1) immediatly after the photoinduced electron transfer step. This proton transfer yields the semiquinone and is driven by a change in pK of the quinone upon formation of the anion radical.

$$\text{C-P}^{\bullet+}\text{-Q}^{\bullet-}\cdots\text{HOOC} \rightarrow \text{C-P}^{\bullet+}\text{-Q}^{\bullet}\text{H}\cdots{}^{-}\text{OOC} \qquad (1)$$

For thermodynamic reasons, electron-hole recombination between the porphyrin radical cation and the semiquinone is expected to be slower than recombination involving the quinone radical anion (*vide infra*). Retarding electron-hole recombination should lengthen the lifetime of the porphyrin radical cation, enhance the yield of electron donation to it by the attached carotenoid, and thus increase the yield of the final charge-separated state C$^{\bullet+}$-P-Q$^{\bullet}$-H$\cdots{}^{-}$OOC.

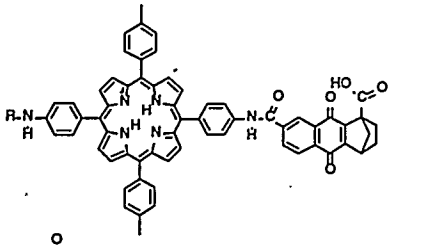

2 R = 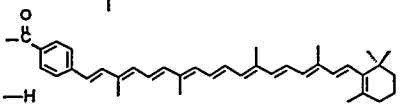

6 R = —H

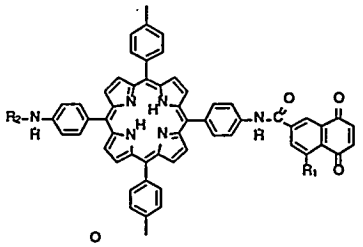

3 R_1 = —Cl R_2 = 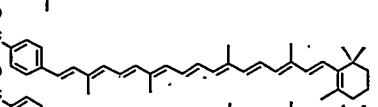

4 R_1 = —H R_2 = 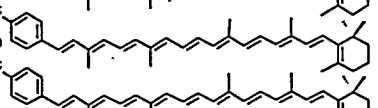

5 R_1 = —OH R_2 =

7 R_1 = —Cl R_2 = —H

8 R_1 = —H R_2 = —H

9 R_1 = —OH R_2 = —H

The quinone moiety of triad **2** has been designed to accomplish this by positioning a carboxylic acid group so that an internal hydrogen bond can form to a carbonyl group of the quinone (shown schematically as Q$\cdots$HOOC). This internal hydrogen bond positions the proton for ultrafast transfer.

Triad **2** is also designed to explore one way to couple a photoinduced electron transfer process to a change in proton chemical potential. Eqs 2 and 3 illustrate two processes involved in the decay of the final charge separated state to the ground state.

$$C^{\bullet+}\text{-P-Q}^{\bullet}H\cdots{}^{-}OOC \rightarrow C\text{-P-Q}^{+}H\cdots{}^{-}OOC \quad (2)$$

$$C\text{-P-Q}^{+}H\cdots{}^{-}OOC \rightarrow C\text{-P-Q}\cdots HOOC \quad (3)$$

The electron-hole recombination reaction shown in eq 2 is a one or two step intramolecular redox process and yields the ground electronic state of the system and the protonated quinone, a highly energetic species. This electron transfer step poises the system for the proton transfer process shown in eq 3 in which the energy change is given by the change in pKa of the relevant proton-bearing species. For triad **2** this energy change is *ca.* 0.7 eV.[12,14]

2. Synthesis

The structural units in the triads and dyads were linked via amide bonds. There are two alternative routes for constructing the triad molecules: coupling the quinone moiety with the porphyrin followed by joining the dyad with the carotenoid polyene, or coupling the porphyrin with the carotenoid polyene and then attaching the quinone. The first approach was used in each of the examples of this study.

3. Absorption Spectra

The absorption spectra in the visible and near UV of **2-9** are essentially linear combinations of those of their component chromophores, indicating that the interchromophore interactions are weak. In the IR region, the spectra are a sensitive function of hydrogen bonding involving the quinone carbonyl group. FT IR spectra were recorded and used to evaluate intramolecular hydrogen bonding between the carboxylic acid group and the carbonyl oxygen in the naphthoquinone moiety in triad **2** and dyad **6**. The IR spectrum of a model compound for the quinone moiety of **2** and **6**, 1-carboxy-1,2,3,4-tetrahydro-1,4-methanoanthracene-9,10-dione, in dilute (0.004 M) dichloromethane solution displayed quinone carbonyl stretching bands at 1665 cm^{-1} and 1630 cm^{-1}. The 1665 cm^{-1} band is assigned to non-hydrogen-bonded quinone carbonyls because it is observed in the methyl ester derivative (1-carbomethoxy-1,2,3,4-tetrahydro-1,4-methanoanthracene-9,10-dione) at 1665 cm^{-1} and in 1,2,3,4-tetrahydro-1,4-methanoanthracene-9,10-dione at 1661 cm^{-1}. The shift to lower frequency resulting in the 1630 cm^{-1} band is characteristic of the shift observed when carbonyl groups are involved in a hydrogen bond.

The IR spectra of the model compound for the quinone moiety of **2** and **6** in dilute dichloromethane solution are interpreted in terms of an equilibrium mixture of internally hydrogen bonded conformers and a population of conformers in which the carboxyl group is rotated so that the internal hydrogen bond is not formed. Because the absorption strengths of the two bands are not known, it is not possible to estimate the value of the equilibrium constant from the IR spectra. It is assumed that these salient features of hydrogen bonding in the model can be extrapolated to triad **2** and dyad **6**.

4. Fluorescence

The fluorescence of **2-9** derives from the porphyrin moiety and is essentially indistinguishable from that of the porphyrin model except for a reduction in quantum yield. Fluorescence decay measurements of **2-9** were obtained in dichloromethane,

chloroform, and benzonitrile with laser excitation at 590 nm. Table 1 presents the fluorescence lifetimes and initial amplitudes for triads **2** - **5** in these solvents. The decays were measured at six wavelengths in the 650-750 nm region and analyzed globally. In the case of triad **3**, for example, a satisfactory fit ($\chi^2 = 1.14$) to the data in benzonitrile was obtained with four exponential components. The major component (93%) has a lifetime of 55 ps. This is much shorter than the *ca.* 10 ns excited singlet state lifetime of the porphyrin, or the 2.5 ns lifetime of the excited singlet porphyrin in a carotenoporphyrin which serves as a model for the linked carotenoid-porphyrin components of triad **3**. Thus, the 55 ps component is one consequence of a new decay pathway in compounds in which a porphyrin and quinone are linked together: electron transfer to the attached quinone acceptor.

Table 1 Fluorescence lifetimes and amplitudes of triads **1** - **4** in various solvents.

Triad	2	3[a]	4[b]	5[b]
τ_f in $CHCl_3$	9 ps (77%) 49 ps (22%)	25 ps	41 ps	9 ps
τ_f in CH_2Cl_2	17 ps (88%) 76 ps (11%)	30 ps	67 ps	11 ps
τ_f in PhCN	51 ps (69%) 157 ps (23%)	55 ps	109 ps	25 ps

[a] A single exponential component accounted for more than 90% of the decay.
[b] A single exponential component accounted for more than 96% of the decay.

In the case of triad **2**, a satisfactory fit to the data ($\chi^2 = 1.15$) was also obtained with four exponential components. However, in this case there are two main exponential components to the decay. The major component, 51 ps (69%), is assigned to the internally hydrogen bonded form of the triad while the 157 ps (23%) component is assigned to conformers in which the carboxylic group is rotated so that hydrogen bonding with the quinone carbonyl does not occur. The component with the shorter lifetime is assigned to the hydrogen bonded conformer because hydrogen bonding is expected to stabilize the quinone anion radical and thereby increase the driving force for electron transfer, which increases the rate. This assignment is bolstered by considering the rate of photoinduced electron transfer in reference dyads **8** and **9**. Dyad **9** exhibits internal hydrogen bonding between the *peri* hydroxyl group and the naphthoquinone so that its quinone has a more positive reduction potential (-0.40 V *vs* SCE) than that of the quinone moiety of dyad **8** (-0.58 V *vs* SCE). As expected, photoinduced electron transfer in **9** is faster than in **8**, as evidenced by the porphyrin fluorescence lifetime of 28 ps in benzonitrile for **9** vs. 113 ps in the same solvent for **8**. Extrapolating the behavior for **8** and **9** to the equilibrium mixture of conformers of triad **2**, those having the internal hyrogen bond are assigned to the 51 ps component of the porphyrin singlet decay and those not internally hydrogen bonded give rise to the 157 ps component.

5. Selection of Reference Triad

In order to assess the role of proton transfer in controlling the yield of long-lived charge-separated species in **2**, it is necessary to design a reference triad in which factors other than the proton transfer step which might affect the yields of the various electron

transfer processes are virtually unchanged from those of **2**. These factors comprise structural and thermodynamic features of the triad. Triad **3** meets the required criteria. The chemical linkages between the components are the same in **2** and **3** and therefore the molecules are expected to have similar conformations.

In order to match the energy levels of the initial charge separated species in **2** and the reference triad, and therefore to have the same thermodynamics for charge recombination from this intermediate, it was necessary to consider the electrochemical potential of the process in eq 4.

$$Q\cdots HOOC + 1e^- \rightarrow Q^{\bullet -}\cdots HOOC \qquad (4)$$

Standard electrochemical techniques cannot resolve this process, and yield only the potential for reduction to the semiquinone species, $Q^{\bullet}$-H···$^{-}$OOC. The strategy employed herein to determine the potential of this step was to synthesize a porphyrin-quinone dyad in which the porphyrin singlet lifetime was about the same as that in dyad **6**, but which could not form intramolecular hydrogen bonds. Given that the other factors controlling electron transfer in the two dyads are the same, equal porphyrin fluorescence lifetimes, and therefore equal electron transfer rate constants, would imply similar thermodynamics for the photoinduced electron transfer step.

6. Time Resolved Absorption

In order to assess the effect of hydrogen bonding and putative proton transfer on the lifetime of the intermediate state C-$P^{\bullet +}$-$Q^{\bullet}$-H···$^{-}$OOC in triad **2**, transient absorption studies with excitation by *ca.* 200 fs pulses at 590 nm were used to directly probe transient state(s) formed upon photoexcitation of dyads **6 - 9** in benzonitrile solution. Dyads **6 - 9** are model compounds for the porphyrin-quinone components of triads **2 - 5**, respectively. As discussed above, dyad **7**, which lacks the internal hydrogen bond, is the appropriate reference compound.

Table 2. Fluorescence lifetimes and decay times of the charge separated states in dyads **6 - 9** in benzonitrile solution.

Dyad	**6**	**7**	**8**	**9**
τ_f (ps)	43, 183[a]	41	113	28
τ_{decay} (ps)	35	33	121	38

[a] As was the case for triad **2**, the longer lived component is assigned to a conformer of **6** in which the internal hydrogen bond is not formed.

By comparison with other PQ systems, the spectra obtained between 624 nm and 766 nm are assigned to the absorption of $^1P^*$ and $P^{\bullet +}$. For dyads **6 - 9**, the spectra in this region rise rapidly and decay more slowly. Global analysis of the decays (Table 2) yields time constants of 35, 33, 121, and 38 ps (major component) for **6**, **7**, **8** and **9**, respectively. These are similar (within experimental error) to those observed from fluorescence decay measurements (43 (and 183), 41, 113 and 28 ps) and therefore report the time constants for the formation of the charge-separated intermediates. As a general rule, the fluorescence lifetime will match either the observed rise or decay time of the transient

absorption associated with the intermediate, and represents the formation time of the intermediate.[7]

A single rise time of < 300 fs was observed for **7** and **8**. By contrast, dyads **6** and **9** exhibited rise times having a longer component . In the case of **7** and **8** the rise time corresponded to the instrument response function, indicating that the decay of $P^{\bullet+}$ is faster than 300 fs. The rise time of the signal for **6** required a two-exponential fit: a 300 fs component and a second component of 3.8 ps. The slow component of the rise of transient absorption in dyad **9** was fitted with a time constant of 810 fs. In **6** and **9** the slower component of the rise time is assigned to the decay of $P^{\bullet+}$. The faster component of the rise in dyad **6** is assigned to the prompt formation of $^1P^*$ and the decay of $P^{\bullet+}$ in conformers lacking the internal hydrogen bond.

These results demonstrate that the lifetime of $P^{\bullet+}$ is longer for the dyads in which the quinone bears a proton donor group, and thus electron-hole recombination is slower. Furthermore, $P^{\bullet+}$ is longer lived in dyad **6**, in which the quinone bears the stronger acid. Similar slow electron-hole recombination in the triads should lead to an increased yield of electron donation by the attached carotenoid. Therefore, the yield of the final charge separated species ($C^{\bullet+}$-P-$Q^{\bullet}$-H·· $^{-}$OOC for **2** and $C^{\bullet+}$-P-$QH^{\bullet}$···$^{-}$OR for **5**) was expected to be greater in triads **2** and **5** than in either **3** or **4**.

7. Energetics and Quantum Yields

The energy diagram in Scheme 1 includes the species important to this work. The energy levels were estimated using appropriate model compounds. These energy estimates are not corrected for Coulombic effects, which are expected to be relatively minor in benzonitrile. The dotted arrows indicate electron transfer reactions and the hollow arrows denote proton transfer processes.

The quantum yields and lifetimes of the final charge-separated species in triads **2** - **5** were determined by monitoring the carotenoid radical cation absorption at 950 nm following excitation at 650 nm. The amplitudes of the transient absorptions at 950 nm are proportional to the relative quantum yields of $C^{\bullet+}$-P-$Q^{\bullet-}$. By the comparative method, the yield of the final charge separation is 22% in the case of triad **2** and 10% in the case of

Table 3 Quantum yields and lifetimes of long-lived charge separated species of triads in dilute benzonitrile solution.

Triad	2	3	4	5
Quantum yield	0.22	0.10	0.11	0.16
Lifetime (ns)	233 & 2500[a]	62	60	70

[a] The decay of the transient absorption of the carotenoid radical cation at 960 nm was fitted as the sum of two exponentials; it is likely that the long-lived component involves bimolecular processes and is only approximated as an exponential.

triad **3**. In fact, as shown in Table 3, the yield for the formation of the final charge separated species $C^{\bullet+}$-P-$^{Q\bullet-}$ is larger in the case of **2** than for any of the triads **3** - **5** and the lifetime of the final charge-separated state is longer in the case of **2** than for any of the reference triads.

Scheme 1

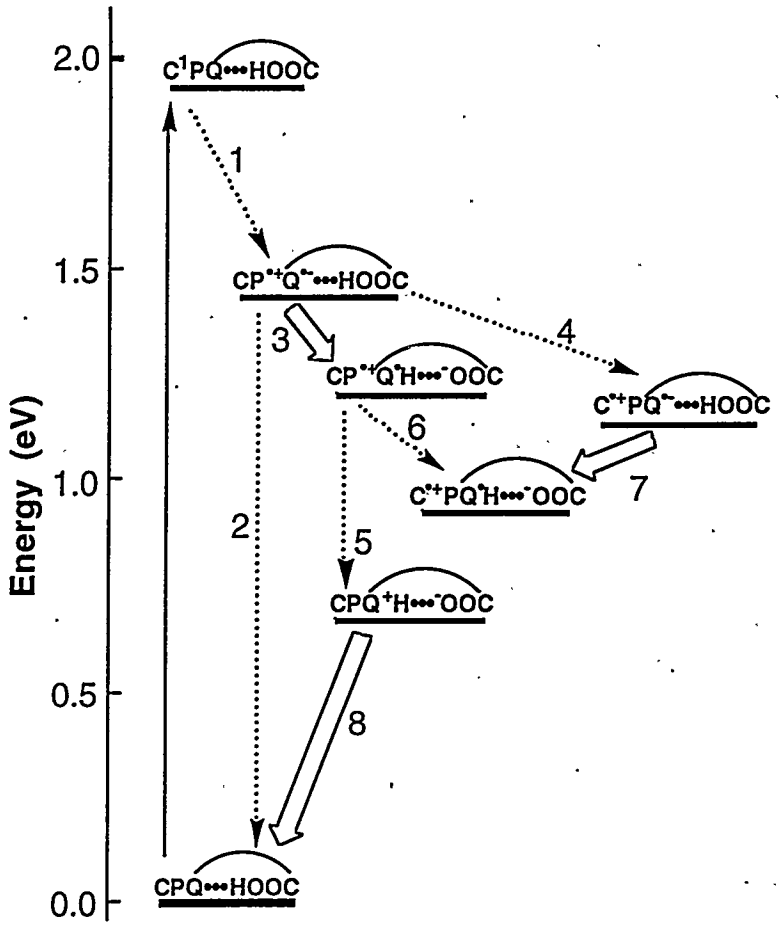

The increased yield of long-lived charge-separation in triad **2** can be interpreted in terms of the chemically relevant species and processes shown in the energy diagram above. Following excitation, the initial charge separated state ($C\text{-}P^{\bullet+}\text{-}Q^{\bullet-}\cdots HOOC$) is generated. Because the lifetime of the charge-separated state $P^{\bullet+}\text{-}Q^{\bullet-}$ in dyad **7** was less than the instrument response time, the rate constant for electron-hole recombination from $C\text{-}P^{\bullet+}\text{-}Q^{\bullet-}\cdots HOOC$, k_2, was estimated[7] to be 4×10^{12} s^{-1}. The driving force for step 2, 1.43 eV, is probably greater than the reorganization energy in these systems and therefore beyond the maximum of the Marcus rate *vs* free energy curve. Competing with this recombination reaction are steps 3 and 4. Step 3 is the proton transfer process wherein the carboxylic acid proton is transferred to the quinone radical anion yielding $C\text{-}P^{\bullet+}\text{-}QH^{\bullet}\cdots{}^{-}OOC$, the semiquinone and the carboxylate moieties. The rate constant for step 3 (and step 7 which is the same proton transfer process) can be calculated from the quantum yield expression in eq 5, which assumes that the yield of step 7 is unity (*vide infra*) and yields $k_3 \sim 1 \times 10^{12} s^{-1}$. Correcting the calculation to allow for the observation that only 70% of **1** is in the hydrogen bonded form yields $k_3 \sim 2 \times 10^{12} s^{-1}$.

$$F(C^{\bullet+}\text{-}P\text{-}Q^{\bullet}\text{-}H\cdots{}^{-}OOC) = 0.22 = k_4/(k_4+k_3+k_2) + \{k_3/(k_4+k_3+k_2)\}\{k_6/(k_6+k_5)\} \quad (5)$$

Steps 4 and 6 involve electron transfer from the carotenoid to the porphyrin radical cation, and to a first approximation are assumed to be equal. In a closely related system this rate constant has been determined to be *ca.* 5×10^{11} s^{-1}. The electron-hole recombination reaction from C-$P^{\bullet+}$-$Q^{\bullet}$-H···$^{-}$OOC, step 5, yields C-P-Q^{+}-H···$^{-}$OOC, a very energetic species. The driving force for step 5 is 0.56 eV. Because ΔG^{0} for step 5 is much less than the reorganization energy in these systems (*ca* 1 eV), step 5 is low in the Marcus normal region and therefore expected to be much slower than recombination by step 2. Indeed, the rate constant for step 5 can be estimated as 3×10^{11} s^{-1} from the lifetime of $P^{\bullet+}$-$Q^{\bullet}$-H···$^{-}$OOC in dyad **6**. Thus, proton transfer shifts electron-hole recombination from a high rate slightly in the Marcus inverted region for the species C-$P^{\bullet+}$-$Q^{\bullet-}$···HOOC to a lower rate in the normal region for the species C-$P^{\bullet+}$-$Q^{\bullet}$-H···$^{-}$OOC.

From ratios of quantum yield expressions (eq 5) for triads **2** and **3** and the rate constants calculated above, it is possible to compare the yields of key pathways in the two triads. Numerical evaluation of these ratios requires the assumption that the yield of step 7 is unity. This is reasonable as the lifetime of analogous charge separated states in triads lacking proton transfer is at least 70 ns and proton transfer is subpicosecond in triad **2**. Because the yield of photoinduced electron transfer (step 1) is essentially unity, the yield of electron donation to the porphyrin radical cation by the carotenoid in **3**, which is analogous to step 4 for triad **2**, determines the yield of long lived charge separated species in triad **3**. This yield is 0.11 in **3** and 0.66 in **2**. The 6-fold increase is attributable to the reduced electron-hole recombination rate resulting from the proton transfer process. The yields for pathways 3 and 4 are 0.2 and 0.09, respectively, indicating that the extremely rapid charge recombination, step 2, accounts for *ca.* 70% of the decay of the initial charge-separated species. By contrast, in model triad **3** the analogous electron-hole recombination accounts for *ca.* 90% of the decay.

8. Conclusions

The coordinated electron transfer-proton transfer process demonstrated by **2** is a viable strategy for increasing the yield of forward electron transfer in multistep systems. Interestingly, in triad **2** a substantial fraction of the intramolecular redox potential from the photoinduced electron transfer process has been translated into a pK difference. Of the 0.9 eV of intramolecular redox energy in the species $C^{\bullet+}$-P-$Q^{\bullet}$H···$^{-}$OOC, approximately 0.64 eV is conserved as proton chemical potential in the species C-P-Q^{+}-H···$^{-}$OOC which formed after the electron-hole recombination process.

The results of this study have been published or are pending publication.[12,14] This system serves as a paradigm for the coupling of electron transfer to a change in proton chemical potential which could ultimately be translated into the generation of proton motive force in a heterogeneous system with appropriate electron and proton transfer relays.

D. Generation and Quenching of Singlet Oxygen by Chlorophyll Aggregates

Chlorophyll triplet states are a byproduct of natural photosynthetic energy conversion. They are formed, for example, by charge recombination of electron transfer

intermediates in reaction centers. Chlorophyll triplets are dangerous because they readily sensitize the formation of singlet molecular oxygen through an energy transfer process. Singlet oxygen is highly reactive, and will destroy the organism unless it has some sort of photoprotection, such as that provided by carotenoid polyenes through quenching of chlorophyll triplet states and/or singlet oxygen itself. The situation is complicated by the fact that chlorophyll itself can quench singlet oxygen, as well as produce it.

In order to learn how to design new photoprotective strategies for artificial photosynthetic systems, we have investigated the ability of both monomeric and aggregated bacteriochlorophyll (BChl) to produce and quench singlet oxygen in model systems and in chlorosome antennas isolated from the green photosynthetic bacterium *Chlorobium vibrioforme* f. *thiosulfatophilum*. Both the chlorosomes and Bchl solutions in certain organic solvents demonstrate a high degree of pigment aggregation, whereas BChl in other solvents exists as monomers or as dimers. The yield of singlet-oxygen photogeneration by pigment dimers was about 6 times less than that of monomers. Singlet oxygen formation was not observed in oligomer-containing solutions or in chlorosomes. To estimate the efficiency of singlet oxygen quenching an effective rate constant for $^1O_2$ quenching by BChl molecules (k^M_q) was determined using the Stern-Volmer equation and the total concentration of BChl *d* in the samples. In solutions containing only monomeric BChl, the k^M_q values coincide with the actual rate constants for $^1O_2$ quenching by BChl molecules. Aggregation weakly influenced the k^M_q values in pigment solutions. In chlorosomes (which contain both BChl and carotenoids) the k^M_q value was less than in solutions of BChl alone and much less than in acetone extracts from chlorosomes. Thus, $^1O_2$ quenching by BChl and carotenoids is much less efficient in chlorosomes than in solution and is likely caused primarily by BChl molecules which are near the surface of the large chlorosome particles. The data allow a general conclusion that monomeric and dimeric chlorophyll molecules are the most likely sources of $^1O_2$ formation in photosynthetic systems. Excitation energy trapping by the long wavelength aggregates as well as $^1O_2$ physical quenching by monomeric and aggregated chlorophyll can be considered as parts of the natural protective system against singlet oxygen formation. This protective effect might be applicable as well to artificial antenna systems in photochemical solar energy harvesting arrays. This work has now been published.[9]

E. Artificial Reaction Centers With Fixed Molecular Geometries

Some of the most intriguing aspects of photoinduced electron transfer in photosynthetic reaction centers are the rapidity of the process in the relatively rigid protein matrix and its apparent insensitivity to temperature and thermodynamic driving force. In contrast, the majority of photosynthetic model systems display photoinduced electron transfer rates that are strong functions of driving force and environmental factors. Most also have molecular structures in which the donor-acceptor electronic interactions are subject to modification by internal rotations.

Covalently linked porphyrin-quinone dyads constitute one of the most thoroughly investigated classes of photosynthetic models. Essentially all of these molecules include at least one single bond in the linkage between the two moieties. Rotation about such bonds can modulate the electronic interactions between the porphyrin electron donor and the quinone acceptor and thus affect the electron transfer rates, which depend strongly

upon such interactions. The presence of single bonds usually introduces ambiguities concerning the most stable molecular conformation, the nature of any transient conformations from which electron transfer may occur, and the effects of intramolecular motions upon observed electron transfer rate constants.

In some cases, the effects of such motions have been reduced by rigidly linking a quinone acceptor to an aryl group that is attached by a single bond to a *meso*-position on the porphyrin macrocycle. Such aryl groups oscillate about the single bond, and the rotation modulates internuclear separations and orientations and therefore the electronic coupling between the ring and the macrocycle. This rotation may be limited by placing substituents at the pyrrole β-positions flanking the aryl ring. The resulting steric hindrance reduces rotational motions about the single bond, but may not completely eliminate them.

In addition, most porphyrin-quinone model systems exhibit photoinduced electron transfer rates that depend upon temperature and the reaction medium. In fact, electron transfer is usually not observable at low temperatures, whereas in reaction centers the process occurs at liquid helium temperatures. As mentioned above, however, photosynthetic photoinduced electron transfer rates evidently depend only weakly on both driving force and temperature.

In order to explore these effects more thoroughly, we have designed a new class of porphyrin-quinone dyads that feature both rigid, non-conjugated hydrocarbon bridges between the donor and acceptor and relatively strong electronic coupling between these moieties, and therefore might be expected to display enhanced electron transfer rates in viscous, non-polar media and at low temperatures. The first of these molecules, dyads **10** - **12**, feature porphyrin electron donor and quinone acceptor moieties that are joined by short bicyclic bridges.

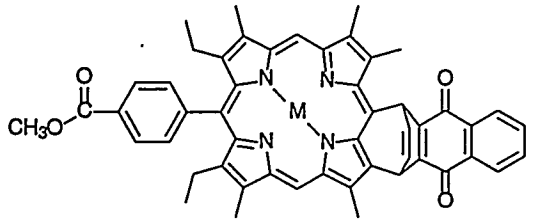

10 : M = H_2
11 : M = Zn

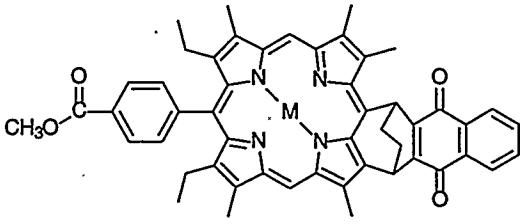

12 : M = H_2

The photochemistry of these dyads was investigated using time-resolved fluorescence and absorption techniques. In all three molecules, photoinduced electron transfer from the porphyrin first excited singlet state to the quinone occurs with rate constants of ~10^{12} s^{-1} in solvents ranging in dielectric constant from ~2.0 to 25.6 and at temperatures from 77 K to 295 K (Table 4). The transfer rate is also relatively insensitive to thermodynamic driving force: photoinduced electron transfer rates for dyad **11** are nearly the same as those for **10** even though the free energy change for photoinduced electron transfer is 0.4 eV larger. This general behavior is phenomenologically similar to photosynthetic electron transfer. The rapid rate of photoinduced electron transfer and its lack of dependence on environmental factors suggests that transfer is essentially independent of solvent and other environmental factors, and is governed by

intramolecular vibrations. Charge recombination of $P^{\bullet+}$-$Q^{\bullet-}$, on the other hand, is substantially slower than charge separation, and sensitive to both driving force and environmental conditions. Thus, by changing conditions, charge recombination rates can be varied over a wide range while photoinduced electron transfer rates are relatively unaffected. This suggests that rigid dyads of this general type may be useful building blocks for more complex molecular devices. This phase of the work has now been published.[13]

The peculiar behavior of these dyads was probed further by synthesis and study of dyad **13**, which differs significantly from **10 - 12** only in that the quinone oxygens have been moved to the adjacent ring of the naphthyl skeleton. Dyad **13** has a similar donor-acceptor linkage to that in **10**, and the redox properties of the porphyrin donor and quinone acceptor are similar, but the quinone carbonyl groups are ~2 Å farther from the porphyrin. The electron transfer rate constants for **10** and **13** are compared in Table 5. In **13**, photoinduced electron transfer rate constants decrease with decreasing solvent dielectric constant. In addition, electron transfer ceases at ~100 K, where the solvent turns

Table 4. Time constants for the rise and decay of the charge-separated state in porphyrin-quinone dyads **10 - 12** as a function of solvent.

	ε	dyad **10**		dyad **11**		dyad **12**	
solvent		k_{rise} (s^{-1})	k_{decay} (s^{-1})	k_{rise} (s^{-1})	k_{decay} (s^{-1})	k_{rise} (s^{-1})	k_{decay} (s^{-1})
benzonitrile	25.60	8×10^{11}	2×10^{11}	3×10^{12}	3×10^{11}	1×10^{12}	2×10^{11}
dichloromethane	9.08	3×10^{12}	5×10^{11}	5×10^{12}	7×10^{11}		
methyltetrahydrofuran	7.60	1×10^{12}	8×10^{10}	5×10^{12}	2×10^{11}	8×10^{11}	7×10^{10}
benzene	2.28	7×10^{12}	4×10^{10}	4×10^{12}	9×10^{10}	2×10^{12}	3×10^{10}
decalin[a]	~2.0			6×10^{12}	5×10^{9}		

[a] This solvent was a ~50:50 mixture of *cis* and *trans* decalin.

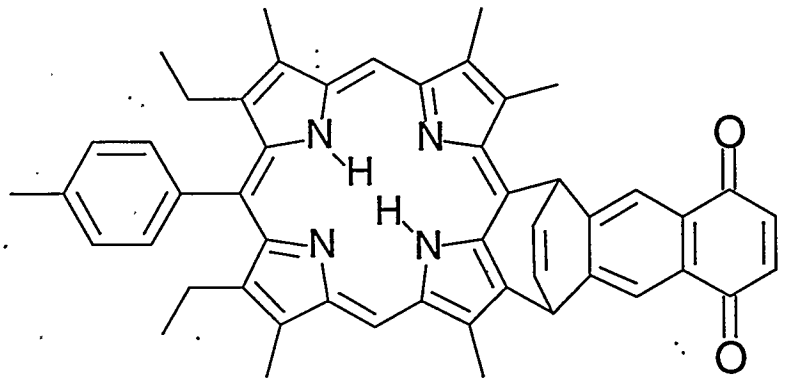

13

Table 5. Rate constants for the rise and decay of the charge-separated state in porphyrin-quinone dyads **10** and **13** as a function of solvent.

		dyad **10**		dyad **13**	
solvent	ε	k_{rise} (s^{-1})	k_{decay} (s^{-1})	k_{rise} (s^{-1})	k_{decay} (s^{-1})
benzonitrile	25.60	8×10^{11}	2×10^{11}	1×10^{12}	2×10^{11}
dichloromethane	9.08	3×10^{12}	5×10^{11}	1×10^{12}	5×10^{11}
2-methyltetrahydrofuran	7.60	1×10^{12}	7.7×10^{10}	1×10^{11}	4.9×10^{10}
toluene	2.38	1×10^{12}	4.4×10^{10}	8.0×10^{10}	9.0×10^{9}
benzene	2.28	7×10^{12}	4.2×10^{10}	2×10^{11}	1.2×10^{10}

to a rigid glass. Thus, electron transfer in **13** exhibits the usual dependence on free energy change and solvent reorganization energy predicted by standard electron transfer theories. Comparison with the results for **13** demonstrates that the anomalous behavior of **10** and its relatives is not due to differences in electronic coupling or to optical electron transfer. It can be attributed at least in part to the smaller separation of the centers of charge of the porphyrin radical cation and the quinone radical anion. The dielectric continuum model suggests that at such short separations relative to the ionic radii, the effective solvent reorganization energy drops to nearly zero and changing the solvent dielectric constant also has no effect on the free energy change for the reaction. Thus, photoinduced electron transfer is insulated from solvent effects, and becomes an intramolecular relaxation process. This second phase of the study has been completed and the results submitted for publication.[15]

The high yield of photoinduced electron transfer in **10** under all conditions and the relatively long lifetime of the charge separated state suggested that dyads such as **10** might be good candidates for elaboration into more complex artificial reaction centers. This was attempted by synthesis and study of triad **14**, which features the porphyrin-quinone dyad architecture of **10**. The porphyrin moiety of **14** was excited, and the

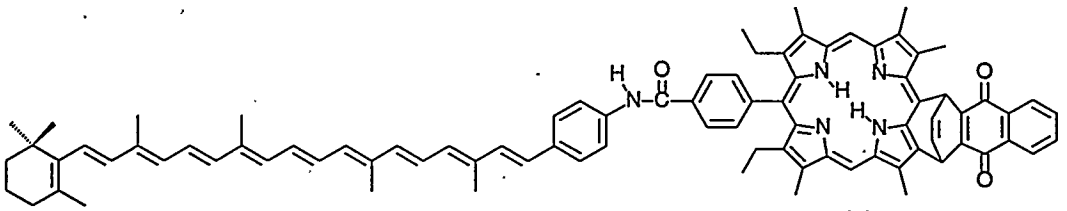

14

porphyrin first excited singlet state was found to be strongly quenched in all solvents investigated. Thus, the C-^{1}P-Q state was converted in high yield into C-$P^{\bullet+}$-$Q^{\bullet-}$. However, transient absorption experiments failed to find evidence for evolution of the initial state into a final $C^{\bullet+}$-P-$Q^{\bullet-}$ state in any solvent other than benzonitrile. In this solvent, the carotenoid radical cation was detected spectroscopically, but in extremely low yield. Thus, electron donation from the carotenoid to the porphyrin radical cation is too slow to compete with recombination of C-$P^{\bullet+}$-$Q^{\bullet-}$.

Several factors may contribute to the failure of **14** to give long-lived charge separation. In nonpolar solvents, the lifetime of C-$P^{\bullet+}$-$Q^{\bullet-}$ is relatively long (Table 4), but stabilization of C-$P^{\bullet+}$-$Q^{\bullet-}$ relative to $C^{\bullet+}$-P-$Q^{\bullet-}$ may make electron transfer from the

carotenoid slow or even endergonic. In polar solvents, the lifetime of $C\text{-}P^{\bullet+}\text{-}Q^{\bullet-}$ is much shorter, and rapid electron transfer from the carotenoid is necessary to achieve the final state in good yield. Two structural features of **14** may lead to slow electron transfer from the carotenoid: steric hindrance to conjugation by the "β-pyrrole" alkyl substituents and the sense of the amide linkage joining the carotenoid and the porphyrin. The importance of these two factors was investigated in the studies described in the next two sections.

F. Effects of Steric and Electronic Factors and Intramolecular Motion on Photoinduced Electron Transfer

1. Steric and Electronic Factors

Meso-tetraarylporphyrins have often been used as components of molecules that mimic photosynthetic reaction centers by carrying out photoinduced electron transfer reactions. In most of these systems, electron transfer is mediated by the covalent linkage joining the donor and acceptor moieties. Many of the model systems involve a porphyrin *meso*-aryl ring in this linkage. In porphyrins with unsubstituted "β-pyrrolic" peripheral positions (*cf.* structure **17**), these aryl rings make angles $\geq 45°$ but $< 90°$ with the mean porphyrin plane. Thus, conjugation between the ring and the macrocycle π-electron system can play a role in the donor-acceptor electronic interaction, which in turn affects the electron transfer rate.

A number of investigators have attempted to limit this conjugative interaction by placing alkyl groups at the β-pyrrolic positions. It is said that the steric effect of these groups forces the aryl ring to be orthogonal to the porphyrin plane, and thus eliminates π-π interactions. There are factors that argue against complete orthogonality; the porphyrin macrocycle might distort significantly due to the steric hindrance, rotational motion on an appropriate time scale about the single bond joining the aryl ring to the macrocycle might significantly populate conformations with π-π overlap, and solution conformations might not demonstrate true orthogonality, as this would force the system to forgo all resonance stabilization.

A second question involves the role of amide bonds in the donor-acceptor linkages. It has been found that a porphyrin linked to a benzoquinone derivative by an amide group having the nitrogen bonded to the porphyrin *meso*-aryl ring (as in **17**) undergoes photoinduced electron transfer 12 times more rapidly than a similar porphyrin-quinone dyad in which the amide linkage has been reversed. A theoretical explanation for this difference has been reported, but it is not clear whether this is a general phenomenon. Both of these structural features are found in triad **14**, and this may contribute to the lack of a significant yield of $C^{\bullet+}\text{-}P\text{-}Q^{\bullet-}$ in that molecule. In order to further investigate these questions, we have prepared and studied the photochemistry of carotene-porphyrin-quinone triads **15** - **17** and related model compounds. Triads **16** and **17** differ in that **16** has sterically demanding methyl groups in the porphyrin β-pyrrolic positions, whereas **17** does not. Triads **15** and **16** differ only in the sense of the amide bond joining the porphyrin and the carotenoid polyene.

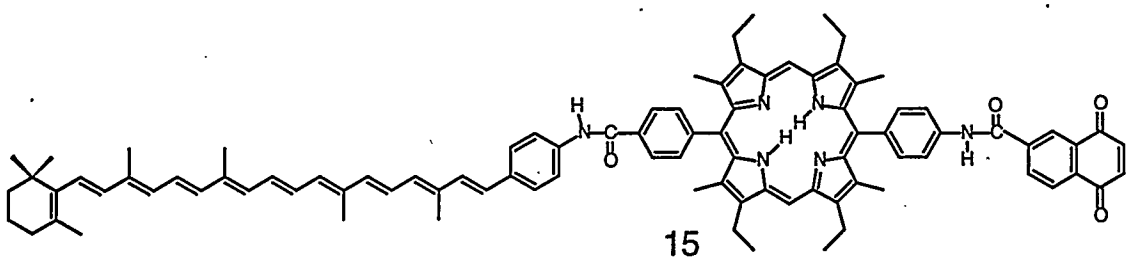

15

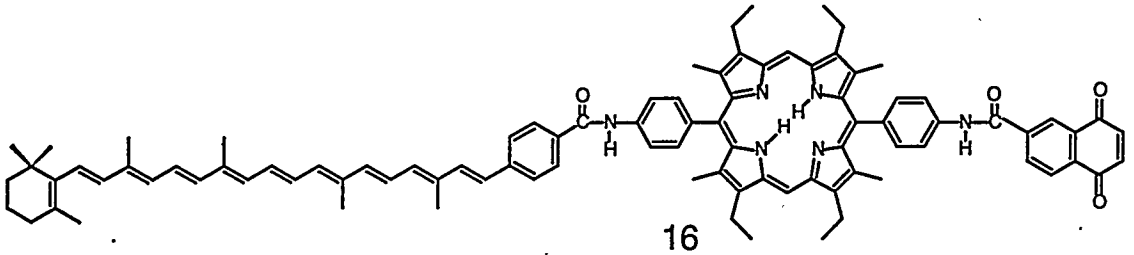

16

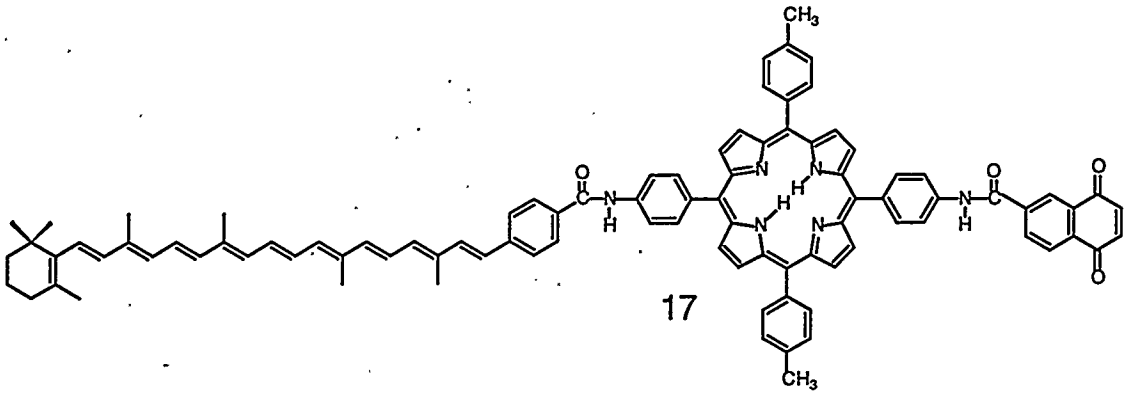

17

The three molecules were studied spectroscopically in benzonitrile using steady-state and transient absorption and emission techniques. The results of these studies were interpreted in terms of Scheme 2, which shows the relevant energy levels and interconversion pathways. In the Scheme, the solid rectangles represent the energy levels for triad **16**, the hollow rectangles those of **15**, and the broken rectangles the energy levels for **17**. The rate constants and quantum yields for the various electron transfer steps are collected in Table 6.

Table 6. Rate constants and quantum yields for triads **15** -**17** in benzonitrile.

Compound	k_1 (s^{-1})	k_2 (s^{-1})	k_3 (s^{-1})	k_4 (s^{-1})	k_5 (s^{-1})	$\Phi_{C\text{-}P^{\bullet+}\text{-}Q^{\bullet-}}$	$\Phi_{C^{\bullet+}\text{-}P\text{-}Q^{\bullet-}}$
15	1.4×10^8	1.1×10^{10}	5.2×10^{11}	3.7×10^{10}	3.8×10^6	0.96	0.064
16	1.6×10^8	9.5×10^9	5.2×10^{11}	2.3×10^{10}	3.2×10^6	0.98	0.042
17	4.6×10^8	8.6×10^9	4.2×10^{12}	2.1×10^{11}	1.5×10^7	0.95	0.046

It will be noted that the rates of photoinduced charge separation (k_2) and the quantum yields of the final $C^{\bullet+}$-P-$Q^{\bullet-}$ states are very similar for the three molecules. This might seem to suggest that structural and electronic changes have no appreciable effect on the photochemistry. However, this is not the case. As shown in the Scheme, the energetics of the molecules differ, and differences in free energy changes lead to

Scheme 2

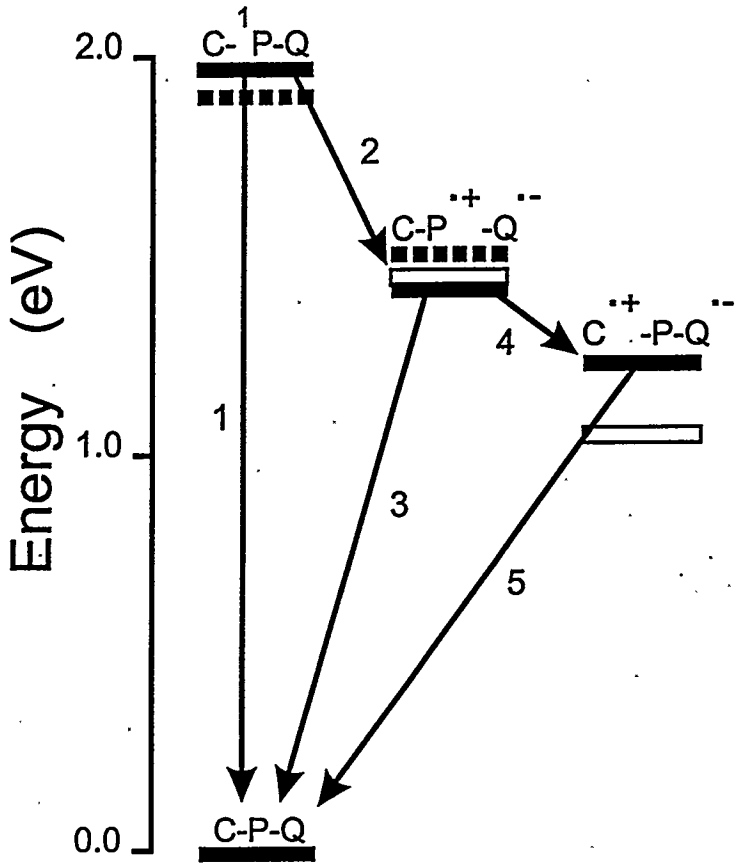

differences in electron transfer rate constants as predicted by Marcus theory. The effect of free energy changes of these magnitudes on electron transfer rate constants is known quantitatively from experiments with other porphyrin-quinone dyad systems. When these effects are included in the analysis, it is found that steric hindrance due to methyl groups at the β-pyrrolic positions reduces electron transfer rate constants by a factor of ~5, relative to hydrogen atoms at these same positions. In addition, amide-containing donor-acceptor linkages having the amino group attached to the porphyrin *meso*-aryl ring demonstrate electron transfer rate constants ~20 times larger than those for similar linkages with the amide reversed, after correction for thermodynamic effects. The results of this study have been submitted for publication.[18]

2. Intramolecular Motions

The study summarized above indicates that steric effects of alkyl groups flanking porphyrin *meso*-aryl substituents at the β-pyrrolic positions slow electron transfer to or from attached donors and acceptors that proceeds via superexchange-mediated electronic coupling through the aryl ring. The effect, however, is relatively small - a factor of about 5. One might expect a larger effect if the flanking groups actually constrain the aryl groups to be orthogonal to the porphyrin macrocycle and thus totally eliminate π-π interactions between the two systems. One possibility is that even in the presence of flanking alkyl groups, the aryl rings are not held rigidly perpendicular to the porphyrin macrocycle, but rather undergo librational motions and sample angles other than 90°. If

such motions occur on the appropriate time scale, they could affect or even control electron transfer rates.

In order to investigate this possibility, we have used ^{13}C NMR spectroscopy to investigate internal motions in porphyrins **18 - 20**. Motions that reorient the C-H bond vector relative to the spectrometer magnetic field can cause relaxation of polarized ^{13}C nuclei, if they are of the correct frequency. Thus, a study of ^{13}C dipole-dipole spin-lattice relaxation times (T_1) can yield information concerning these motions.

Such studies were carried out in deuteriochloroform solution at 303 K at a field strength of 11.7 T. The results appear in Table 7. Looking at the table, it is evident that in all three molecules, the spin-lattice relaxation times for the Ar2, Ar3, Ar5 and Ar6 carbon atoms are longer than those for the Ar4 carbons and the carbon atoms at the periphery of the porphyrin macrocycle. This indicates that internal motion about the bonds linking the aryl rings to the macrocycle occurs, and is rapid enough to affect relaxation.
Quantitative analysis of the results allowed determination of the overall diffusion coefficient for reorientation of the porphyrin macrocycle (tumbling as an isotropic rotor), D_0, and the diffusion coefficients for internal rotation about the bonds joining the aryl groups to the macrocycle, D_1. The overall reorientation of all three porphyrins occurs with

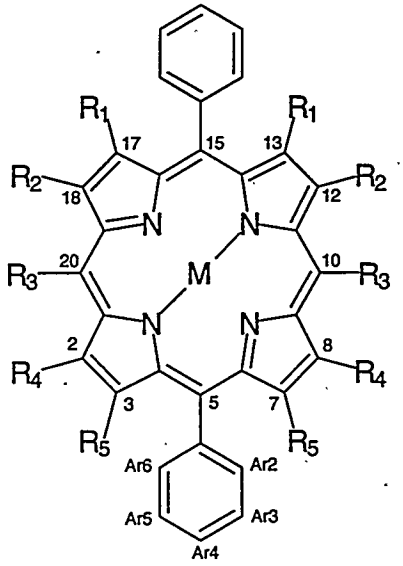

18: $R_1 = R_2 = R_4 = R_5 = H$, $R_3 =$  , $M = H_2$

19: $R_1 = R_5 = CH_3$, $R_2 = R_4 = CH_2CH_3$, $R_3 = H$, $M = H_2$

20: $R_1 = R_2 = R_3 = H$, $R_4 = (CH_2)_5CH_3$, $R_5 = CH_3$, $M = Zn$

$D_0 \sim 1 \times 10^9\ s^{-1}$. In porphyrins with only hydrogen at the β-pyrrolic positions, the *meso* phenyl rings undergo rotations about their single bonds to the porphyrin with $D_1 \sim 4 \times 10^9\ s^{-1}$. Introduction of methyl substituents at the β-pyrrolic positions adjacent to the phenyl rings reduces these motions, but only to $\sim 1 \times 10^9\ s^{-1}$. Thus, significant internal motions are present in both types of molecules. These motions occur on the time scale of many

photoinduced electron and energy transfer processes in porphyrins covalently linked to electron or energy donors or acceptors through *meso* aryl groups. Thus, the internal librational motions may affect rates of photoinduced electron and energy transfer, even in relatively "rigid" molecular constructs. This work has been submitted for publication.[17]

Table 7: Selected Carbon-13 Chemical Shifts and Spin-Lattice Relaxation Times for Porphyrins 18 - 20 in Deuteriochloroform at 303 K

Carbon	Porphyrin 18[a]		Porphyrin 19		Porphyrin 20	
	δ (ppm)	T_1 (s)	δ (ppm)	T_1 (s)	δ (ppm)	T_1 (s)
2, 8	131.1	0.45±0.04	---	---	---	---
3, 7	131.1	0.45±0.04	---	---	---	---
10, 20	---	---	96.5	0.52±0.02	102	0.38±0.06
12, 18	131.1	0.45±0.04	---	---	132	0.40±0.03
13, 17	131.1	0.45±0.04	---	---	131	0.40±0.03
5Ar2,6	134.6	0.72±0.01	133.1	0.58±0.01	133	0.48±0.02
15Ar2,6	134.6	0.72±0.01	133.1	0.58±0.01	135	0.61±0.02
5Ar3,5	126.7	0.72±0.01	127.6	0.57±0.01	127.6	0.46±0.01
15Ar3,5	126.7	0.72±0.01	127.6	0.57±0.01	126.6	0.60±0.03
5Ar4	127.7	0.46±0.01	128.3	0.46±0.01	128.3	0.39±0.01
15Ar4	127.7	0.46±0.01	128.3	0.46±0.01	127.3	0.41±0.04

[a] For porphyrin **18**, the chemical shifts and T_1 values for the carbon atoms of the phenyl groups at the 10 and 20 positions are identical to those reported for the corresponding carbon atoms of the phenyl rings at the 5 and 15 positions, for reasons of symmetry.

III. Publications and Meeting Presentations Resulting from the Project

This list reports all publications since those included in the previous Technical Progress Report (1993)

A. Publications

1. "Mimicking Photosynthetic Energy and Electron Transfer," D. Gust, T. A. Moore and A. L. Moore, *Photochemical and Photoelectrochemical Conversion and Storage of Solar Energy,* Z. W. Tian and Y. Cao, eds. (Beijing: International Academic Publishers), 113-119 (1993).

2. "Molecular Mimicry of Photosynthetic Energy and Electron Transfer," D. Gust, T. A. Moore and A. L. Moore, *Accounts of Chemical Research*, **26**, 198 - 205 (1993).

3. "The Photochemistry of Carotenoids. Some Photosynthetic and Photomedical Aspects," D. Gust, T. A. Moore, A. L. Moore, J. Jori and E. Reddi, *Ann. New York Acad. Sci.*, **691,** 32-48 (1993).

4. "Photoinitiated Charge Separation in a Carotenoid-Porphyrin-Diquinone Tetrad: Enhancement of Quantum Yields via Control of Electronic Coupling," S.-J. Lee, J. M. DeGraziano, A. N. Macpherson, E.-J. Shin, G. R. Seely, P. K. Kerrigan, A. L. Moore, T. A. Moore and D. Gust, *Chem. Phys.*, **176,** 321 - 336 (1993).

5. "Photoinduced Electron and Energy Transfer in Molecular Pentads," D. Gust, T. A. Moore, A. L. Moore, A. N. Macpherson, A. Lopez, J. M. DeGraziano, I. Gouni, E. Bittersmann, G. R. Seely, F. Gao, R. A. Nieman, X. C. Ma, L. Demanche, D. K. Luttrull, S.-J. Lee and P. K. Kerrigan, *J. Am. Chem. Soc.,* **115,** 11141 - 11152 (1993).

6. "Photosynthesis Mimics as Molecular Electronic Devices," D. Gust, T. A. Moore and A. L. Moore, *IEEE Engineering in Medicine and Biology Magazine*, **13**, 58 - 66, (1994).

7. "Kinetics of Multistep Photoinitiated Electron Transfer Reactions in a Molecular Triad," S.-C. Hung, S. Lin, A. N. Macpherson, J. M. Degraziano, P. K. Kerrigan, P. A. Liddell, A. L. Moore, T. A. Moore and D. Gust, *J. Photochem. Photobiol. A: Chem.,* **77,** 207 - 216 (1994).

8. "Carotenoids: Nature's Unique Pigments for Light and Energy Processing," T. A. Moore, D. Gust and A. L. Moore, *Pure & Appl. Chem.*, **66**, 1033-1040 (1994).

9. "Generation and Quenching of Singlet Molecular Oxygen by Aggregated Bacteriochlorophyll-*d* in Model Systems and Chlorosomes," A. A. Krasnovsky, Jr., J.

Lopez, P. Cheng, P. A. Liddell, R. E. Blankenship, T. A. Moore and D. Gust, *Photosynthesis Research,* **40**, 191 - 198 (1994).

10. "Molecular Wires and Girders," D. Gust, *Nature*, **372,** 133 - 134 (1994).

11. "Molecular Approaches to Artificial Photosynthesis," D. Gust, T. A. Moore and A. L. Moore, in *Alternative Fuels and the Environment,* F. S. Sterrett, ed. (Chelsea, MI: Lewis Publishers,), 125 - 139 (1995).

12. "Coordinated Photoinduced Electron and Proton Transfer in a Molecular Triad," S.-C. Hung, A. N. Macpherson, S. Lin, P. A. Liddell, G. R. Seely, A. L. Moore, T. A. Moore and D. Gust, *J. Am. Chem. Soc.*, **117**, 1657 - 1658 (1995).

13. "Ultrafast Photoinduced Electron Transfer in Rigid Porphyrin-Quinone Dyads," A. N. Macpherson, P.A. Liddell, S. Lin, L. Noss, G. R. Seely, J. M. DeGraziano, A. L. Moore, T. A. Moore and D. Gust, *J. Am. Chem. Soc.*, **117**, 7202 - 7212 (1995).

14. "Photoinduced Electron and Proton Transfer in a Molecular Triad," S.-C. Hung, A. N. Macpherson, S. Lin, P. A. Liddell, G. R. Seely, A. L. Moore, T. A. Moore and D Gust, *Photochemistry and Radiation Chemistry: Complementary Methods for the Study of Electron-Transfer,* ACS Advances in Chemistry Series, (Washington DC: American Chemical Society) in press.

15. "Contrasting Photoinduced Electron Transfer Properties of Two Closely Related Rigidly-Linked Porphyrin-Quinone Dyads," J. P. Sumida, P. A. Liddell, A. N. Macpherson, G. R. Seely, A. L. Moore, T. A. Moore and D. Gust, *J. Phys. Chem.*, submitted for publication.

16. "Artificial Photosynthetic Reaction Centers in Liposomes: Photochemical Generation of Transmembrane Proton Potential," G. Steinberg-Yfrach, P. A. Liddell, S.-C. Hung, A. L. Moore, D. Gust and T. A. Moore, submitted for publication.

17. "Aryl Ring Rotation in Porphyrins. A Carbon-13 NMR Spin-Lattice Relaxation Time Study," L. Noss, P. A. Liddell, A. L. Moore, T. A. Moore and D. Gust, submitted for publication.

18. Structural Effects on Photoinduced Electron Transfer in Carotenoid-Porphyrin-Quinone Dyads," D. Kuciauskas, P. A. Liddell, S.-C. Hung, Su Lin, S. Stone, G. R. Seely, A. L. Moore, T. A. Moore and D. Gust, submitted for publication.

B. Meeting Presentations

19. "Photoinduced Electron Transfer in Synthetic Tetrads and Pentads," D. Gust, T. A. Moore and A. L. Moore, Seventeenth DOE Solar Photochemistry Research Conference, Brainerd, MN, June, 1993.

20. "Photoinduced Electron Transfer in Model Systems for Photosynthesis," D. Gust, T. A. Moore, A. L. Moore, NATO Advanced Research Workshop on Photoinduced Electron Transfer Reactions, Albufeira, Portugal, September, 1993.

21. "Artificial Photosynthesis," D. Gust, Second Nordic Congress on Photosynthesis, Oslo, Norway, November, 1993.

22. "Mimicking Photosynthetic Electron and Energy Transfer," T. A. Moore, D. Gust and A. L. Moore, Fourth Annual Symposium on Photoinduced Charge Transfer, Rochester, NY, July, 1993.

23. "Electron Transfer to Hydrogen Bonded Quinone Systems," A. L. Moore, T. A. Moore, D. Gust, S.-C. Hung, A. Macpherson, P. K. Kerrigan and J. M. DeGraziano, Fourth Annual Symposium on Photoinduced Charge Transfer, Rochester, NY, July, 1993.

24. "Synthesis and Photochemistry of a Molecular Triad. Electron Transfer to a Hydrogen Bonded Quinone System," S.-C. Hung, A. N. Macpherson, P. K. Kerrigan, J. M. DeGrazaino, A. L. Moore, T. A. Moore and D. Gust, 206th National Meeting of the American Chemical Society, Chicago, IL, 1993.

25. "Photophysics of Porphyrin-Quinone Molecules with Fixed Molecular Geometry," P. Liddell, S. Lin, A. N. Macpherson, J. M. DeGraziano, G. Seely, A. L. Moore, T. A. Moore and D. Gust, XVIth International Conference on Photochemistry, Vancouver, Canada, August, 1993.

26. "Carótenoporphyrins: Models for the Carotenoid Function in Photosynthesis," S. Cardoso, T. A. Moore, A. L. Moore and D. Gust, Third Annual Western Regional Photosynthesis Conference, Asilomar, CA, January, 1994.

27. "Mimicking Photosynthetic Electron and Energy Transfer," T. A. Moore, D. Gust and A. L. Moore, IV Encuentro Latinoamericano / I Iberoamericano de Fotoquímica y Fotobiología, Valparaíso, Chile, April, 1994.

28. "Biomedical Applications of Carotenoporphyrins," A. L. Moore, T. A. Moore and D. Gust, IV Encuentro Latinoamericano / I Iberoamericano de Fotoquímica y Fotobiología, Valparaíso, Chile, April, 1994.

29. "Increased Yield of Long-Lived Charge Separation Resulting from Protonation of an Electron Transfer Intermediate," S.-C. Hung, A. Macpherson, A. L. Moore, T. A. Moore and D. Gust, Eighteenth DOE Solar Photochemistry Research Conference, Tahoe City, CA, June, 1994.

30. "The Triplet Energy of a Carotenoid Pigment Determined by Photoacoustic Calorimetry," J. E. Lewis, D. Benin, D. Nicodem, S. Nonell, A. L. Moore, D. Gust, and T. A. Moore, Twentysecond Annual Meeting of the American Society for Photobiology, Scottsdale, AZ, June, 1994. (*Photochem. Photobiol.*, **59S**, 35S, (1994)).

31. "Electron Transfer in Porphyrin-Quinone Molecules With Fixed Molecular Geometry," P. Liddell, S. Lin, A. N. Macpherson, J. M. DeGraziano, G. Seely, A. L. Moore, T.A. Moore and D. Gust, Twentysecond Annual Meeting of the American Society for Photobiology, Scottsdale, AZ, June, 1994 (*Photochem. Photobiol.* **59S,** 19S (1994)).

32. "Electron Transfer to Hydrogen Bonded Quinone Systems," A. L. Moore, T. A. Moore, D. Gust, S.-C. Hung and A. N. Macpherson, Twentysecond Annual Meeting of the American Society for Photobiology, Scottsdale, AZ, June, 1994 (*Photochem. Photobiol.* **59S,** 45S (1994)).

33. "Carotenoporphyrins: Models for the Carotenoid Function in Photosynthesis," S. L. Cardoso, T. A. Moore, A. L. Moore and D. Gust, Twentysecond Annual Meeting of the American Society for Photobiology, Scottsdale, AZ, June, 1994 (*Photochem. Photobiol.* **59S,** 92S (1994)).

34. "Generation and Quenching of Singlet Molecular Oxygen by Aggregated Bacteriochlorophyll-D in Model Systems and Chlorosomes," A. A. Krasnovsky, Jr., J. Lopez, P. Cheng, P. A. Liddell, R. E. Blankenship, T. A. Moore and D. Gust, Twentysecond Annual Meeting of the American Society for Photobiology, Scottsdale, AZ, June, 1994 (*Photochem. Photobiol.* **59S,** 94S (1994)).

35. "Carotenoids as Photoprotective and Localizing Agents in Tumor Imaging," A. L. Moore, T. A. Moore and D. Gust, Gordon Research Conference on Lasers in Medicine and Biology, Meriden, NH, July, 1994.

36. "Coupled Electron and Proton Transfer Processes in Model Systems," S.-C. Hung, A. N. Macpherson, S. Lin, G. R. Seely, A. L. Moore, T. A. Moore and D. Gust, Gordon Research Conference on Photosynthesis, Biophysical Aspects, New Hamption, NH, August, 1994.

37. "Carotenoporphyrins: Models for the Carotenoid Function in Photosynthesis," S. L. Cardoso, D. E. Nicodem, T. A. Moore, A. L. Moore and D. Gust, Gordon Research Conference on Photosynthesis, Biophysical Aspects, New Hamption, NH, August, 1994.

38. "Coupled Electron-Proton Transfer: A Strategy to Enhance the Forward Electron transfer Yield in Multicomponent Systems," S.-C. Hung, A. N. Macpherson, P. A. Liddell, G. R. Seely, A. L. Moore, T. A. Moore and D. Gust, Gordon Research Conference on Electron Donor - Acceptor Interactions, Newport, RI, August, 1994.

39. "Photoinduced Electron Transfer in Photosynthesis Models," D. Gust, T. A. Moore and A. L. Moore, Gordon Conference on Electron Donor-Acceptor Interactions, Newport, RI, August, 1994.

40. "Molecular Approaches to Artificial Photosynthesis," D. Gust, T. A. Moore and A. L. Moore, IX Congreso Argentino de Fisicoquímica, San Luis, Argentina, November, 1994.

41. "Photoinduced Electron and Proton Transfer in a Molecular Triad," S.-C. Hung, A. N. Macpherson, S. Lin, P. A. Liddell, G. R. Seely, A. L. Moore, T. A. Moore and D. Gust, 209th ACS National Meeting, Anaheim, CA, April, 1995.

42. "Photoinduced Electron Transfer in Porphyrin-Quinone Systems: New Strategies for Enhancing Quantum Yields," D. Gust, T. A. Moore, A. L. Moore, Nineteenth DOE Solar Photochemistry Research Conference, Tamiment, PA, June, 1995.

43. "Rigid Porphyrin-Quinone Models for Photosynthetic Electron Transfer," D. Gust, T. A. Moore, A. L. Moore, P. A. Liddell, A. N. Macpherson, J. P. Sumida, S. Lin, G. R. Seely and L. Noss, 23rd Annual Meeting of the American Society for Photobiology, Washington, DC, June, 1995, *Photochem. Photobiol.* **61S,** 59S (1995).

44. "A Photobiochemical Model System for Solar Energy Conversion," T. A. Moore, A. L. Moore and D. Gust, Quinto Simposium de Química: Medicina Molecular, Monterrey, Mexico, September, 1995.

45. "Artificial Photosynthesis," D. Gust, DOE Research Opportunities in Photochemical Sciences Workshop, Estes Park, Colorado, February, 1996.

46. "Porphyrin-Based Mimics of Photosynthetic Reaction Centers," D. Gust, The Royal Society of Chemistry Perkin/Dalton Symposium on Contemporary Aspects of Photochemistry, Birmingham, UK, March, 1996.

47. "Artificial Photosynthesis: Mimicking Biological Solar Energy Conversion," T. A. Moore, D. Gust and A. L. Moore, 3rd Annual Nebraska Metallobiochemistry Retreat, Lincoln, Nebraska, April, 1996.

48. "Photoinduced Electron Transfer and Correlated Proton Transfer in Supramolecular Devices," A. L. Moore, D. Gust and T. A. Moore, 3rd Annual Nebraska Metallobiochemistry Retreat, Lincoln, Nebraska, April, 1996.

49. "Solar Energy Conversion by Artificial Photosynthesis," T. A. Moore, D. Gust and A. L. Moore, Primera Semana De La Facultad De Ciencias, Universidad Autónoma Del Estado De Morelos, Cuernavaca, Mexico, May, 1996.

50. "Photochemistry of Artificial Reaction Centers in Liposomes. Transmembrane Proton Transfer," Twenty-Fourth Annual Meeting of the American Society for Photobiology, Atlanta, GA, June, 1996, *Photochem. Photobiol.* **63S,** 21S - 22S (1996).

51. "Photochemistry of Artificial Reaction Centers in Liposomes. Transmembrane Proton Transfer," G. Steinberg-Yfrach, P. A. Liddell, S.-C. Hung, A. L. Moore, D. Gust and T. A. Moore, 20th DOE Solar Photochemistry Conference, French Lick, Indiana, June, 1996.